DOI: 10.1002/ejic.201000974

Reactivity of Dinuclear Copper(I)/pybox Complexes towards Isocyanides and Phosphanes

María Panera,[a] Josefina Díez,[a] Isabel Merino,[b] Eduardo Rubio,[a,b] and M. Pilar Gamasa*[a]

Dedicated in memory of Professor José Manuel Concellón

Keywords: Copper / Isocyanide ligands / Phosphane ligands / Pybox complexes

The dinuclear complexes $[Cu_2(R\text{-pybox})_2][PF_6]_2$ {R-pybox = 2,6-bis[4′-(*S*)-isopropyloxazolin-2′-yl]pyridine for (*S*,*S*)-*i*Pr-pybox (**1**) and 2,6-bis[4′-(*R*)-phenyloxazolin-2′-yl]pyridine for (*R*,*R*)-Ph-pybox (**2**)} are very efficient precursors for the synthesis of dinuclear and mononuclear derivatives containing isocyanide or phosphane ligands. The reaction of **1** and **2** with the isocyanides (CNBn or CNCy) resulted in the synthesis of the dinuclear derivatives $[Cu_2(R\text{-pybox})_2(CNBn)_2][PF_6]_2$ [R-pybox = (*S*,*S*)-*i*Pr-pybox (**3**), (*R*,*R*)-Ph-pybox (**4**)] and $[Cu_2(R\text{-pybox})_2(CNCy)_2][PF_6]_2$ [R-pybox = (*S*,*S*)-*i*Pr-pybox (**5**), (*R*,*R*)-Ph-pybox (**6**)]. When the reaction was carried out with the monodentate ($PMePh_2$, PPh_3) and the bidentate phosphanes [dppm, dppf, (*S*)-peap] the mononuclear complexes $[Cu(R\text{-pybox})(PRPh_2)_2][PF_6]$ [R-pybox = (*S*,*S*)-*i*Pr-pybox, R = Me(**7**), Ph (**8**); R-pybox = (*R*,*R*)-Ph-pybox, R = Ph (**9**)], $[Cu(R\text{-pybox})\{(S)\text{-peap}\}][PF_6]$ [R-pybox = (*S*,*S*)-*i*Pr-pybox (**11**), (*R*,*R*)-Ph-pybox (**12**)], and $[Cu(R\text{-pybox})(dppf)][PF_6]$ [R-pybox = (*S*,*S*)-*i*Pr-pybox (**13**), (*R*,*R*)-Ph-pybox (**14**)] and the dinuclear complex $[Cu_2\{(S,S)\text{-}i\text{Pr-pybox}\}(\mu\text{-dppm})_2][PF_6]_2$ (**10**) were obtained, respectively. The structures of complexes **3**, **7**, **10**, and **13** have been resolved by X-ray diffraction methods and by 1D, 2D, and DOSY NMR spectroscopy measurements. The ^1H, ^{31}P, and ^{19}F DOSY NMR spectroscopic experiments provided evidence that the solid-state nuclearity of compounds **3**, **7**, **10**, and **13** is maintained in solution and confirmed that these ionic compounds exist in solution as stable, discrete, cationic complexes.

Introduction

Recent studies on Cu^I-catalyzed asymmetric reactions, such as cyclopropanation,[1] allylic oxidation,[2] azide–alkyne cycloaddition,[3] and alkyne addition to imines,[4] that were carried out using in situ generated copper(I)-pybox catalysts, reflect that the efficiency of the process is highly dependent on the structure of the pybox ligand as well as on the nature of the copper(I) salt employed. In spite of this, a C_2-symmetric tridentate mononuclear complex $[Cu(\kappa^3\text{-}N,N,N\text{-R-pybox})]^+$ has been routinely claimed as the active catalytic species regardless of the copper salt precursor.

Recently, we found that discrete dinuclear complexes like $[Cu_2\{(R,R)\text{-Ph-pybox}\}_2][X]_2$ (X = OTf, PF_6), which are obtained from $CuOTf{\cdot}0.5C_6H_6$ or $[Cu(MeCN)_4][PF_6]$, behave as efficient catalysts for the alkynylation of imines.[5] The dinuclear structure of these derivatives was confirmed in the solid state and in solution by X-ray diffraction studies and by ^1H and ^{19}F DOSY NMR spectroscopy, respectively. We proposed that $[Cu_2(R\text{-pybox})_2][X]_2$ complexes, which contain two equivalent tricoordinate copper centers in the solution state, are the active catalytic species, although the mononuclear species resulting from the dissociation of the former complexes during the catalytic cycle could not be definitively ruled out. In order to continue the study on the reactivity and applications of these complexes, we report herein the reaction of complexes $[Cu_2(R\text{-pybox})_2][X]_2$ [R-pybox = (*S*,*S*)-*i*Pr-pybox, (*R*,*R*)-Ph-pybox; X = OTf, PF_6] with the phosphane and isocyanide ligands that resulted in the formation of novel dinuclear and mononuclear complexes containing the pybox ligand.

Results and Discussion

Firstly, we investigated the reaction of $[Cu_2(R\text{-pybox})_2][PF_6]_2$ [R-pybox = (*S*,*S*)-*i*Pr-pybox (**1**) and (*R*,*R*)-Ph-pybox (**2**)] with anionic ligands, such as NaCl/MeOH and Ph-C≡C-H/KO*t*Bu. While the former anionic ligand produced[5] the dinuclear complex $[Cu_2(\mu\text{-Cl})\{(S,S)\text{-}i\text{Pr-}$

[a] Departamento de Química Orgánica e Inorgánica, Instituto Universitario de Química Organometálica "Enrique Moles" (Unidad Asociada al C.S.I.C.), Universidad de Oviedo, 33071 Oviedo, Spain
Fax: +34-985-103446
E-mail: pgb@uniovi.es
[b] Unidad de Resonancia Magnética Nuclear, Servicios Científico-Técnicos de la Universidad de Oviedo, 33071 Oviedo, Spain
Supporting information for this article is available on the WWW under http://dx.doi.org/10.1002/ejic.201000974.

pybox}$_2$][PF_6], the latter ligand gave a complex mixture from which only [Cu(C≡CPh)]$_n$ could be characterized. At this point, we turned our attention to the behavior of complexes **1** and **2** towards neutral ligands. The reaction of **1** with N-donor ligands like pyridine and 1,10-phenanthroline resulted in the recovery of the starting complex and in the formation of [Cu(phen)$_2$][PF_6], respectively. Therefore, further studies were directed to a different type of ligand, namely the isocyanides and phosphanes.

Reaction of [Cu_2(R-pybox)$_2$][X]$_2$ [R-pybox = (*S*,*S*)-*i*Pr-pybox, (*R*,*R*)-Ph-pybox] with the Isocyanides: The Synthesis of the Dinuclear Complexes [Cu_2(R-pybox)$_2$(CNBn)$_2$][X]$_2$ [X = PF_6, R-pybox = (*S*,*S*)-*i*Pr-pybox (3), (*R*,*R*)-Ph-pybox (4); X = OTf, R-pybox = (*S*,*S*)-*i*Pr-pybox (3a), (*R*,*R*)-Ph-pybox (4a)] and [Cu_2(R-pybox)$_2$(CNCy)$_2$][PF_6]$_2$ [R-pybox = (*S*,*S*)-*i*Pr-pybox (5), R-pybox = (*R*,*R*)-Ph-pybox (6)]

The reaction of [Cu_2(*i*Pr-pybox)$_2$][PF_6]$_2$ (**1**) and [Cu_2(Ph-pybox)$_2$][PF_6]$_2$ (**2**) with the isocyanides RN≡C (R = Bn, Cy) in dichloromethane at room temperature gave rise to the air-stable, yellow solid, dinuclear complexes [Cu_2(R-pybox)$_2$(L)$_2$][PF_6]$_2$ (L = RN≡C)(**3**–**6**) in moderate yield (47–60%) (Scheme 1).

Complexes **3**–**6**, as well as the other complexes reported in this article, have been characterized by IR, NMR spectroscopy, molar conductivity, mass spectroscopy, and/or elemental analysis (see Exp. Section). The molar conductivity values for complexes **3**–**6** are in the range expected for 1:2 electrolytes.[6] Characteristic features of the spectroscopic data are: (i) the IR spectra show the expected absorptions for the PF_6^- anion (ca. 840 cm^{-1}), as well as those characteristic of the ν(C≡N) group (2184–2175 cm^{-1}). The IR spectra of other copper(I) complexes with terminal isocyanide ligands show comparable ν(C≡N) shifts,[7] (ii) the $^{13}C\{^1H\}$ NMR spectra (298 K) show a singlet for the quaternary carbon of *C*NR in the range of 141.8 to 139.7 ppm, and (iii) the mass spectra of complexes **3**–**6** show an intense peak that corresponds to the mass of cation [Cu(R-pybox)(L)]$^+$ (L = CNBn, CNCy). In the mass spectra, the expected Δ*m*/*z* = 0.5 peak separations, which are typical of the doubly charged species [Cu_2(R-pybox)$_2$(L)$_2$]$^{2+}$, are not observed.

The triflate derivatives [Cu_2(R-pybox)$_2$(CNBn)$_2$][OTf]$_2$ [R-pybox = (*S*,*S*)-*i*Pr-pybox (**3a**) and (*R*,*R*)-Ph-pybox (**4a**)] were prepared in the same way from the [Cu_2(R-pybox)$_2$][OTf]$_2$ complexes (see Supporting Information).

Single-crystal X-ray diffraction analysis was performed on complex **3**. An ORTEP-type view of the cationic complex is shown in Figure 1 and selected bonding data are listed in Table 1. The structure shows a dimeric cation

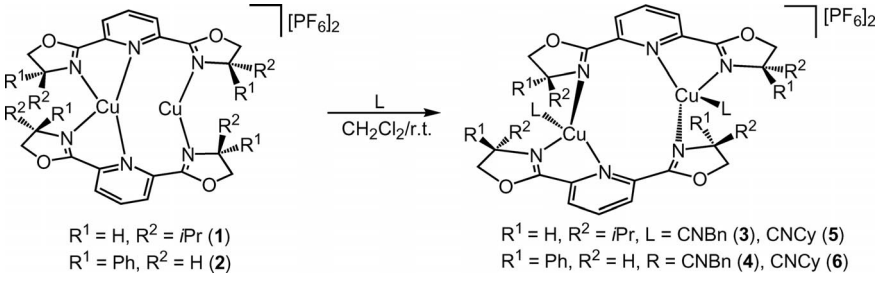

Scheme 1.

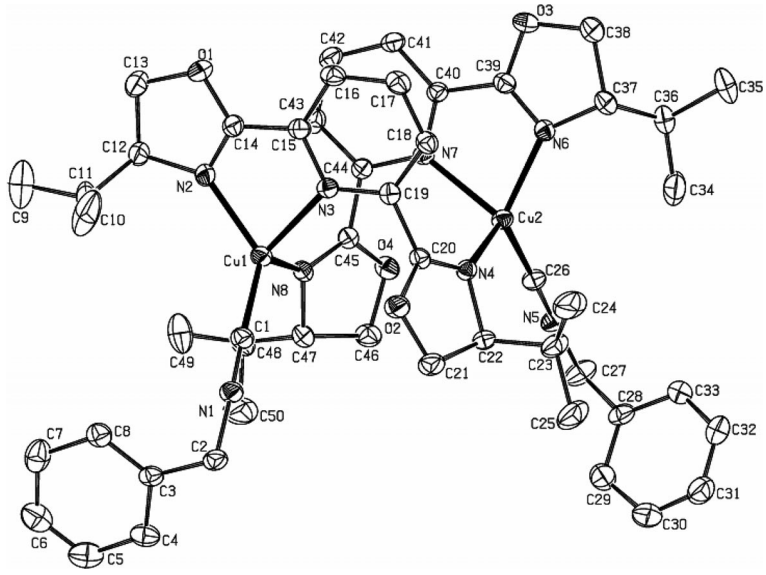

Figure 1. An ORTEP drawing of complex **3** showing the atom labeling scheme. The thermal ellipsoids are shown at 10% probability. The hydrogen atoms and the PF_6^- anions are omitted for clarity.

Table 1. Selected bond lengths [Å] and angles [°] for complexes **3**, **7**, **10**·2CH_2Cl_2·Et_2O, and **13**.

Complex **3**			
Bond		Bond	
Cu(1)–C(1)	1.853(5)	Cu(2)–C(26)	1.873(5)
Cu(1)–N(2)	2.036(4)	Cu(2)–N(6)	2.074(4)
Cu(1)–N(3)	2.171(4)	Cu(2)–N(7)	2.141(3)
Cu(1)–N(8)	2.060(4)	Cu(2)–N(4)	2.052(4)
C(1)–N(1)	1.157(6)	C(26)–N(5)	1.148(6)
Angle		Angle	
Cu(1)–C(1)–N(1)	168.4(5)	Cu(2)–C(26)–N(5)	174.7(4)
C(1)–N(1)–C(2)	174.5(6)	C(26)–N(5)–C(27)	175.4(5)
C(1)–Cu(1)–N(2)	128.07(19)	C(26)–Cu(2)–N(6)	125.35(19)
C(1)–Cu(1)–N(8)	106.37(18)	C(26)–Cu(2)–N(4)	107.84(17)
C(1)–Cu(1)–N(3)	124.1(2)	C(26)–Cu(2)–N(7)	121.75(17)
N(2)–Cu(1)–N(8)	112.10(16)	N(6)–Cu(2)–N(4)	116.11(14)
N(2)–Cu(1)–N(3)	79.19(15)	N(6)–Cu(2)–N(7)	79.11(14)
N(8)–Cu(1)–N(3)	103.34(13)	N(4)–Cu(2)–N(7)	102.46(13)
Complex **7**			
Bond		Bond	
Cu(1)–N(3)	2.045(3)	Cu(1)–P(1)	2.2292(11)
Cu(1)–N(2)	2.348(3)	Cu(1)–P(2)	2.2805(11)
Angle		Angle	
N(3)–Cu(1)–P(1)	119.72(9)	N(3)–Cu(1)–N(2)	77.45(11)
N(3)–Cu(1)–P(2)	104.26(9)	P(1)–Cu(1)–N(2)	123.18(8)
P(1)–Cu(1)–P(2)	126.01(4)	P(2)–Cu(1)–N(2)	94.23(7)
Complex **10**·2CH_2Cl_2·Et_2O			
Bond		Bond	
Cu(1)–N(1)	1.991(5)	Cu(2)–N(2)	2.272(5)
Cu(1)–P(1)	2.2210(16)	Cu(2)–N(3)	2.093(5)
Cu(1)–P(3)	2.2676(18)	Cu(2)–P(2)	2.3237(17)
Cu(1)–Cu(2)	2.7430(11)	Cu(2)–P(4)	2.2980(17)
Angle		Angle	
N(1)–Cu(1)–P(1)	126.75(16)	N(3)–Cu(2)–P(2)	92.41(15)
P(1)–Cu(1)–P(3)	123.54(7)	N(2)–Cu(2)–P(2)	113.04(13)
N(1)–Cu(1)–P(3)	106.02(16)	P(4)–Cu(2)–P(2)	140.29(7)
N(2)–Cu(2)–N(3)	77.25(19)	P(1)–C(55)–P(2)	110.0(3)
N(3)–Cu(2)–P(4)	111.67(15)	P(3)–C(30)–P(4)	110.7(3)
N(2)–Cu(2)–P(4)	103.09(13)		
Complex **13**			
Bond		Bond	
Cu(1)–N(1)	2.330(4)	Cu(1)–P(1)	2.2761(15)
Cu(1)–N(2)	2.068(4)	Cu(1)–P(2)	2.2985(15)
Angle		Angle	
P(1)–Cu(1)–P(2)	115.56(6)	P(2)–Cu(1)–N(2)	120.57(14)
P(1)–Cu(1)–N(1)	120.16(13)	P(2)–Cu(1)–N(1)	93.66(12)
P(1)–Cu(1)–N(2)	119.12(14)	N(2)–Cu(1)–N(1)	78.29(17)

$[Cu_2\{(S,S)$-*i*Pr-pybox$\}_2(CNBn)_2]^{2+}$ and two uncoordinated PF_6^- anions. Each copper atom is bonded to the oxazoline and pyridine nitrogen atoms of one pybox unit and to the oxazoline nitrogen of the other pybox unit. The tetrahedral coordination around each copper is completed by the benzyl isocyanide ligand. The two copper atoms have equivalent distorted tetrahedral arrays and no significant differences between the corresponding distances and angles around each copper atom were found. The bond angles around each copper atom are in the range of 79.19(15) to 128.07(19)° for Cu(1) and 79.11(14) to 125.35(19)° for Cu(2). The pybox skeleton is not planar and has torsion angles of 116.4(5)° [N(3)–C(19)–C(20)–N(4)] and 125.1(4)° [N(7)–C(44)–C(45)–N(8)]. The Cu(1)–Cu(2) bond length (5.175 Å) is elongated compared to that of the precursor complex **1** [2.7292(12) Å], which indicates that no copper–copper interaction is present.

The benzyl isocyanide groups present a distorted linear arrangement [Cu(1)–C(1)–N(1) and Cu(2)–C(26)–N(5) angles of 168.4(5)° and 174.7(4)°, respectively]. These angle values along with the bond lengths for the copper-isocyanide bond [(Cu(1)–C(1), 1.853(5) Å and Cu(2)–C(26), 1.873(5) Å] and for the C≡N bond [(C(1)–N(1), 1.157(6) Å and C(26)–N(5), 1.148(6) Å] are in the range of those found for other copper(I)-isocyanide complexes.[7,8]

The room-temperature ^1H and ^{13}C NMR spectra for complexes **3**–**6** are consistent with the existence of a time-averaged structure presenting a C_2 symmetry axis originating from a rapid pyridine ligand exchange between the two copper atoms. On the other hand, the freezing temperature for the equivalence of both oxazoline groups was found to be 193 K according to the variable temperature (VT) NMR experiments recorded for complex **3** (^1H and ^{13}C NMR; 298–183 K). The ^{13}C NMR spectrum of **3** at 183 K shows that all the signals assigned to the oxazoline carbon atoms, as well as those assigned to the C-2,6 and C-3,5 atoms of the pyridine ring, have been resolved into two sets of peaks, while a single set of signals is observed for the C-4 carbon of the pyridine and for all of the carbon atoms of the two benzyl isocyanide ligands. This new compound was characterized at 183 K by 2D NMR spectroscopy (HSQC, HMBC, and ROESY) (see Supporting Information). From this spectroscopic information it can be deduced that: (i) the rapid pyridine ligand exchange, which makes both of the oxazoline rings of the one pybox ligand equivalent at room temperature, is frozen at 193 K and (ii) at this temperature there is still a symmetry element in the molecule that preserves the equivalence between one half of a pybox unit and the other half of the second pybox unit and that makes the two isocyanide ligands equivalent. On the other hand, the internal fluxional equilibrium of the precursor complex, $[Cu_2\{(S,S)$-*i*Pr-pybox$)_2\}][PF_6]_2$ (**1**), is not frozen when the solution is cooled below 183 K.[5] It can be assumed that the internal fluxional equilibrium may be unfavorable for complex **3**, in contrast to complex **1**, because of the less stable conformation that is imposed by the higher coordination number of the copper atoms.

Reaction of $[Cu_2(R\text{-pybox})_2][X]_2$ with Monodentate Phosphanes: The Synthesis of the Mononuclear Complexes $[Cu(R\text{-pybox})(PRPh_2)_2][X]$ [X = PF_6, R-pybox = (*S*,*S*)-*i*Pr-pybox, R = Me (7), Ph (8); R-pybox = (*R*,*R*)-Ph-pybox, R = Ph (9). X = OTf, R-pybox = (*S*,*S*)-*i*Pr-pybox, R = Me (7a), Ph (8a); R-pybox = (*R*,*R*)-Ph-pybox, R = Ph (9a)]

Complexes **1** and **2** react with the monodentate phosphanes (1:4 molar ratio) in dichloromethane at room temperature to provide the mononuclear complexes [Cu(R-

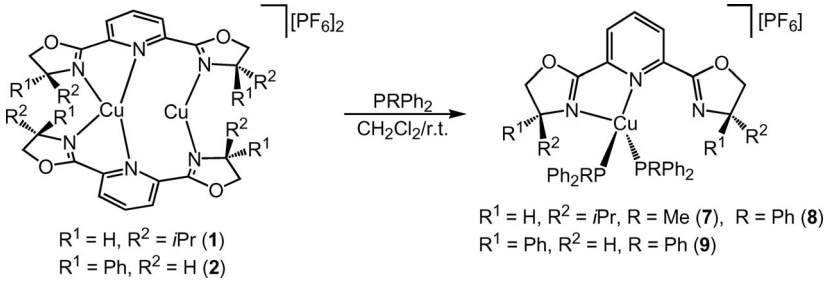

Scheme 2.

pybox)(PRPh$_2$)$_2$][PF$_6$] (**7**–**9**) in good yield (75–76%) (Scheme 2). The molar conductivity values are in the range expected for 1:1 electrolytes.[6] When the reaction was carried out in 1:2 molar ratio, mixtures of complexes **7**–**9** and the precursor complexes were obtained. The triflate complexes, [Cu(R-pybox)(PRPh$_2$)$_2$][OTf] [R-pybox = (*S*,*S*)-*i*Pr-pybox, R = Me (**7a**), Ph (**8a**); R-pybox = (*R*,*R*)-Ph-pybox, R = Ph (**9a**)], were analogously prepared using [Cu$_2$(R-pybox)$_2$][OTf]$_2$ as the precursors (see Supporting Information).

The structure of complex **7** has been confirmed by single-crystal X-ray analysis. An ORTEP-type view of the cationic complex **7** is shown in Figure 2 and selected bonding data are listed in Table 1. The structure of complex **7** shows a mononuclear cation [Cu{(*S*,*S*)-*i*Pr-pybox}(PMePh$_2$)$_2$]$^+$ and an uncoordinated PF$_6^-$ anion. The Cu(1) atom is bonded to the phophorous atom of the two PMePh$_2$ ligands and to the nitrogen of the oxazoline and of the pyridine rings of the pybox ligand and exhibits a very distorted tetrahedral coordination with the bond angles around the copper atom in the range of 77.45(11)° [N(3)–Cu(1)–N(2)] to 126.01(4)° [P(1)–Cu(1)–P(2)]. The Cu–N(pybox) bond lengths are dissimilar. The Cu–N(oxazoline) bond [Cu(1)–N(3), 2.045(3) Å] is much shorter than the Cu–N(pyridine) bond [Cu(1)–N(2), 2.348(3) Å]. The pybox skeleton is not planar and has a torsion angle [N(1)–C(6)–C(7)–N(2)] of –159.4(4)°. The Cu(1)–P bond lengths are similar to those found for other copper(I) complexes containing monodentate phosphane and N-donor ligands.[9]

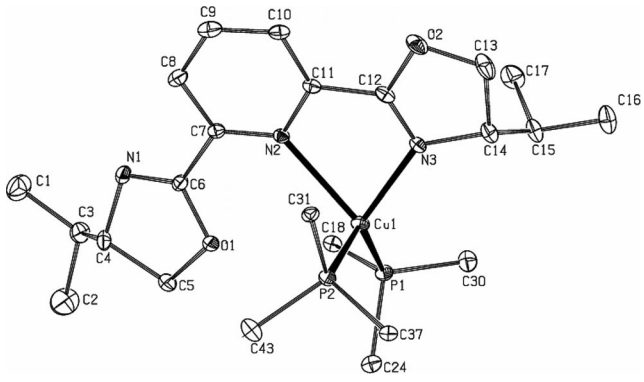

Figure 2. An ORTEP drawing of complex **7** showing the atom labeling scheme. The thermal ellipsoids are shown at 10% probability. The hydrogen atoms and the PF$_6^-$ anion are omitted for clarity.

While the oxazoline rings of complex **7** are not equivalent in the solid state, they become equivalent in solution. Thus, the VT ^{1}H and ^{13}C NMR spectra (298–183 K) are consistent with the existence of a time-averaged structure presenting a C_2 symmetry axis originating from a rapid exchange process (see Supporting Information), as previously observed for the mononuclear complex [Cu(*S*,*S*)-*i*Pr-pybox)$_2$][PF$_6$].[5]

Reaction of [Cu$_2$(R-pybox)$_2$][PF$_6$]$_2$ (1 and 2) with Bidentate Phosphanes: The Synthesis of the Dinuclear [Cu$_2${(*S*,*S*)-*i*Pr-pybox}(μ-dppm)$_2$][PF$_6$]$_2$ (10) and the Mononuclear Complexes [Cu(R-pybox){(*S*)-peap}][PF$_6$] [R-pybox = (*S*,*S*)-*i*Pr-pybox (11), (*R*,*R*)-Ph-pybox (12)] and [Cu(R-pybox)-(dppf)][PF$_6$] [R-pybox = (*S*,*S*)-*i*Pr-pybox (13), (*R*,*R*)-Ph-pybox (14)]

Next, we assessed the reaction of **1** and **2** with three bidentate phosphane ligands, namely bis(diphenylphosphanyl)methane (dppm), (–)-*N*,*N*-bis(diphenylphosphanyl)-(*S*)-1-phenylethylamine [(*S*)-peap], and 1,1′-bis(diphenylphosphanyl)ferrocene (dppf). The two former ligands present a similar small bite angle and are frequently used as bridging ligands to stabilized dimetallic complexes,[10–12] while the latter ligand usually exhibits a chelating ability, although its bridging behavior in dinuclear complexes is also well documented.[13]

The reaction of complex **1** with dppm (1:2 molar ratio) in dichloromethane at room temperature led to complex [Cu$_2${(*S*,*S*)-*i*Pr-pybox}(μ-dppm)$_2$][PF$_6$]$_2$ (**10**) in 67% yield (Scheme 3). The formation of **10** involved replacement of one pybox ligand by two diphosphane ligands that bridge both copper atoms. In contrast, reaction of complexes **1** and **2** with the diphosphanes (*S*)-peap and dppf, under the same reaction conditions, furnished exclusively the mononuclear complexes **11**–**12** and **13**–**14** (48–95% yield), respectively. In this case, the bidentate phosphanes behaved as chelating ligands.

The most characteristic features of the spectroscopic data for complexes **10**–**14** are described below. The ^{31}P{^{1}H} NMR spectra of these complexes exhibit a broad singlet at δ = –3.6 (**10**), 88.2 (**11**), 88.9 (**12**), –12.1 (**13**), and –12.4 (**14**) ppm, which are all downfield compared to that of the corresponding free ligand [dppm (δ = –23 ppm), (*S*)-peap (δ = 55.3 ppm), and dppf (δ = –16.9 ppm)]. The ^{13}C{^{1}H} NMR spectra show signals characteristic of the carbon

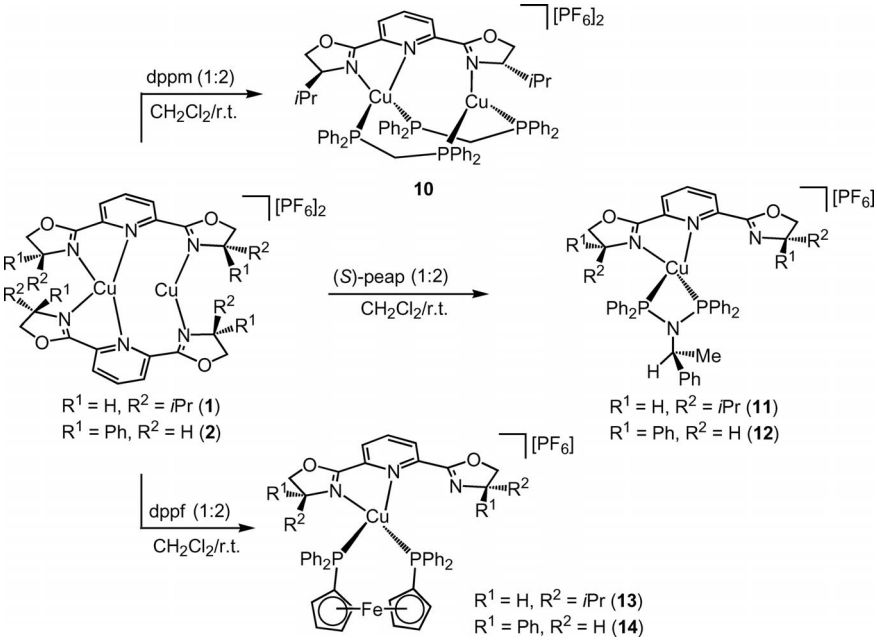

Scheme 3.

atoms of the phosphorus ligands: (i) complex **10** shows a singlet (δ = 26.3 ppm) for the methylene carbon of both dppm ligands, (ii) complexes **11** and **12** exhibit two singlet signals at δ = 62.1, 22.1 (**11**), and 61.2, 21.2 (**12**) ppm for the CH and CH_3 carbons of the NCHMePh group, and (iii) complexes **13** and **14** show signals for the η^5-C_5H_4 rings of the dppf ligand. Moreover, the single set of signals observed for the pybox ligand in complexes **11**–**14** is in accordance with the presence of a C_2 symmetry axis.

Single-crystal X-ray analysis of complexes **10** and **13** have been performed. All attempts to grow crystals of **11** and **12** using different solvent mixtures failed to produce suitable crystals for diffraction study. The ORTEP-type views of the cationic complexes **10** and **13** are shown in Figures 3 and 4,

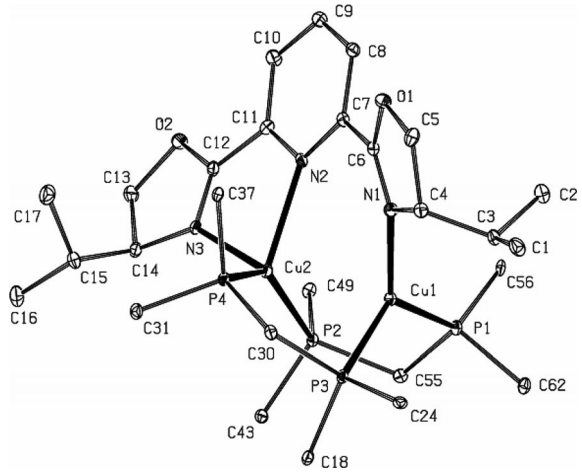

Figure 3. An ORTEP drawing of complex **10** showing the atom labeling scheme. The thermal ellipsoids are shown at 10% probability. The hydrogen atoms and the PF_6^- anions are omitted for clarity. Only the C^{ipso}–aryl atoms of the dppm ligands are drawn.

respectively, and selected bonding data are listed in Table 1. The structure of complex **10** shows a dimeric cation $[Cu_2\{(S,S)$-*i*Pr-pybox$\}(\mu$-dppm$)_2]^{2+}$ and two uncoordinated PF_6^- anions. The two copper atoms of the cation, held in close proximity by one *i*Pr-pybox and two dppm bridging ligands, have different coordination environments, namely tetrahedral and trigonal distorted arrays. Thus, Cu(2) and Cu(1) are coordinated to the nitrogen atoms of the *i*Pr-pybox ligand through the pyridine-oxazoline and oxazoline units, respectively. The coordination around each copper is completed by two phosphorus atoms of the dppm ligands. The Cu–Cu distance [2.7430(11) Å] is consistent with nonbonding Cu–Cu contacts[14] and is similar to that found for the precursor **1** [2.7292(12) Å].[5] Remarkably, the pybox skeleton is not planar with a torsion angle [N(2)–C(7)–C(6)–N(1)] of 31.2(10)°. The Cu–P distance is 2.2776 Å on average, which is comparable to those observed in other dinuclear copper(I) complexes containing μ-dppm ligands.[11]

The structure of complex **13** shows a mononuclear cation $[Cu\{(S,S)$-*i*Pr-pybox$\}$(dppf)$]^+$ and an uncoordinated PF_6^- anion. The Cu(1) atom is bonded to both phosphorus atoms of the dppf ligand and to the oxazoline and the pyridine nitrogen atoms of the pybox ligand in a highly distorted tetrahedral arrangement. Unlike complex **7**, the copper–pyridine nitrogen bond length for complex **13** [Cu(1)–N(2) 2.068(4) Å] is shorter than that of the copper–oxazoline nitrogen bond [Cu(1)–N(1) 2.330(4) Å]. The nonplanar pybox skeleton exhibits a small torsion angle [N(2)–C(7)–C(6)–N(3)] of 22.3(9)°. The bond angles around the copper atom are in the range of 78.29(17)° [N(2)–Cu(1)–N(1)] to 120.57(14)° [N(2)–Cu(1)–P(2)]. The Cu(1)–P(1) [2.2761(15) Å] and Cu(1)–P(2) [2.2985(15) Å] bond lengths and the P(1)–Cu(1)–P(2) bite angle of the chelating dppf ligand [115.56(6)°] are comparable to those observed in

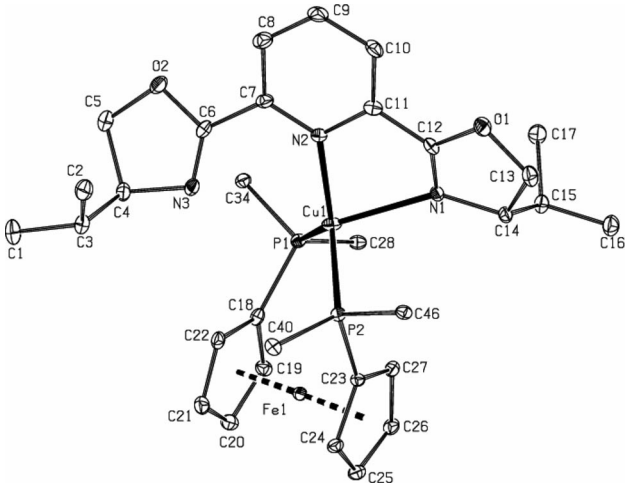

Figure 4. An ORTEP drawing of complex **13** showing the atom labeling scheme. The thermal ellipsoids are shown at 10% probability. The hydrogen atoms and the PF_6^- anions are omitted for clarity. Only the C^{ipso}–aryl atoms of the dppf ligand are drawn. CT01 and CT02 are the centroids of the C(18)–C(22) and C(23)–C(27) rings.

other copper(I) complexes containing dppf ligands.[13a,15] The ferrocenyl C_5H_4 rings are almost parallel [dihedral angle of 2.09(24)°] and adopt a staggered conformation with a torsion angle [C(18)-CT01-CT02–C(23)] of 61.25(72)° (see Figure 4). The mean interplane distance between both rings is 3.29 Å. The Cu···Fe distance [3.8734(32) Å] exceeds the sum of the van der Waals radii (3.40 Å),[16] which indicates that there is no interaction between the copper and iron atoms.

The VT ^{1}H and ^{31}P NMR spectra of complexes **10** and **13** indicate that the internal fluxional process, which is responsible for the equivalence of both oxazoline rings at room temperature, is maintained in the temperature range of 298 to 183 K (see Supporting Information for 2D and VT NMR spectroscopy).

NMR Diffusion Studies

The solid-state characterization of the new pybox copper(I) complexes was complemented with a solution-state study by NMR spectroscopy, which included structure elucidation, variable temperature measurements, and diffusion studies using diffusion ordered spectroscopy (DOSY). The interest in characterizing the species present in solution arises from the potential ability of these compounds to act as catalysts in some organic transformations as has been previously shown for other pybox-containing copper(I) complexes.[1–5]

Our previous NMR spectroscopic and diffusion studies[5] on the precursor dinuclear copper(I) complex, $[Cu_2\{(S,S)$-*i*Pr-pybox$\}_2][PF_6]_2$, showed that the species present in solution are fully consistent with the structure derived from the single-crystal X-ray analysis and that no dissociated or associated species are formed upon dissolution. However, the influence of ligands other than pybox to induce associative or dissociative processes in solution in these copper(I) complexes may not be dismissed. Thus, the presence of complexes with different molecular sizes was studied through diffusion ordered spectroscopy (DOSY).[17] One of the more convenient applications of the diffusion NMR spectroscopy is the estimation of the molecular sizes of the molecules in solution.[18] This technique measures the diffusion coefficient (D) of the molecule in the NMR sample, which is a translational property that can be related to its hydrodynamic radius (r_H) through the Stokes-Einstein equation.[19] Associated or dissociated species that might exist in solution can be detected by comparing this hydrodynamic radius with the radius obtained from the X-ray data, and also valuable information about the interaction between the cations and the anions for the ionic compounds can be obtained.[20]

The complexes **3**, **10**, and **7**, **13** (Figure 5) were chosen for these studies as representative examples of the dinuclear and the mononuclear complexes, respectively. These complexes were subjected to ^{1}H, ^{19}F, and ^{31}P DOSY NMR spectroscopy, which were acquired with the *ledbpgp2s* pulse program. For the ^{1}H DOSY NMR spectroscopy measurements sample spinning was applied to avoid convection influence.[21] The diffusion results obtained for the cationic and the anionic fragments, the hydrodynamic radii afforded via the Stokes–Einstein equation, and the radii calculated from the X-ray structures[22] are presented in Table 2.

The presence of the NMR active nuclei ^{31}P and ^{19}F in the PF_6^- anion enabled the behavior of both the cationic and the anionic fragments in solution to be compared. In all the complexes investigated, the ^{19}F and ^{31}P DOSY NMR spectroscopy afforded a much larger diffusion coefficient for the PF_6^- anions than those obtained from the ^{1}H DOSY NMR spectroscopy for the cations, which suggests that the PF_6^- anions are moving separately and faster than their cationic complexes. This observation is supported by the ^{31}P DOSY NMR spectrum of complex **10** (Figure 6) where the difference between the diffusion coefficient for the PF_6^- anion ($\log D = -8.62\ m^2 s^{-1}$) and for the dppm ligand in the cation fragment ($\log D = -9.02\ m^2 s^{-1}$) is evident.

Consequently, the values for the hydrodynamic radii, calculated from the diffusion coefficients measured in the cationic fragments, account only for the size of the cation complexes and therefore, when compared with the X-ray data, only the cationic radii should be used. There is good agreement between the volume of the cationic complexes in the liquid and in the solid state (see Table 2), which discards the presence of associated or dissociated species in the solution. This information is especially relevant for the dinuclear complex **3** (r_H = 6.75 Å, $r_{X\text{-}ray}$ = 6.82 Å), since its ^{1}H and ^{13}C NMR spectra could also be assigned to a monomer species due to its symmetrical nature. When compared to the previously reported[5] hydrodynamic radii of the dinuclear complex $[Cu_2\{(S,S)$-*i*Pr-pybox$\}_2][PF_6]_2$ (**1**) (r_H = 6.3 Å) and to the mononuclear complex $[Cu\{(S,S)$-*i*Pr-pybox$\}_2][PF_6]$ (r_H = 5.5 Å), the value of r_H for complex **3** is closer to that of a dimeric complex rather than to that

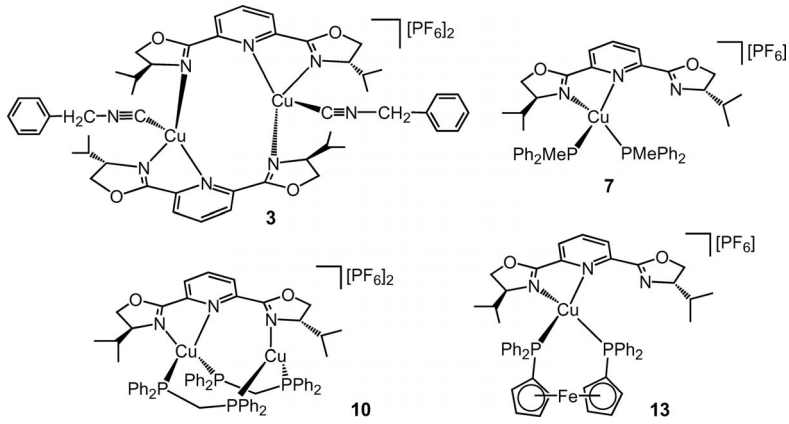

Figure 5. Complexes **3**, **7**, **10**, and **13**.

Table 2.The ^{1}H DOSY, ^{31}P DOSY, and ^{19}F DOSY NMR spectroscopic experiments for complexes **3**, **7**, **10**, and **13**.[a]

	Nucleus	Fragment	log *D* [$m^2 s^{-1}$][b]	*D* ($\times 10^{-9}$) [$m^2 s^{-1}$]	r_H [Å]	$r_{X\text{-ray}}$ [Å][c]
3	^{1}H	cation	–8.99	1.02	6.75	6.82 (7.05)
3	^{19}F	anion	–8.62	2.39	2.88	2.54[d]
7	^{1}H	cation	–8.94	1.15	6.02	6.29 (6.43)
7	^{31}P	anion	–8.60	2.51	2.75	2.54
7	^{19}F	anion	–8.59	2.57	2.68	2.54
10	^{1}H	cation	–9.01	0.98	7.23	7.29 (7.49)
10	^{31}P	cation	–9.02	0.95	7.23	7.29 (7.49)
10	^{31}P	anion	–8.62	2.39	2.88	2.54[c]
10	^{19}F	anion	–8.62	2.39	2.88	2.54
13	^{1}H	cation	–8.96	1.09	6.30	6.47 (6.60)
13	^{31}P	anion	–8.60	2.51	2.84	2.54

[a] η(acetone, 298 K) = 0.000316 kg ms^{-1}. [b] The diffusion coefficients were measured in a logarithmic scale and the accuracy of the reported values are ±0.01 for the ^{1}H DOSY NMR spectra and ±0.02 for the ^{31}P and ^{19}F DOSY NMR spectra. [c] The radii of the cationic complexes were obtained from their X-ray structures and were determined by calculating the volume of the complex and subtracting the volume of the PF_6^- anions. The molecular radii of the complexes, as calculated from the X-ray structures, are shown in parenthesis. [d] The radius of the PF_6^- anion was calculated from its van der Waals volume.

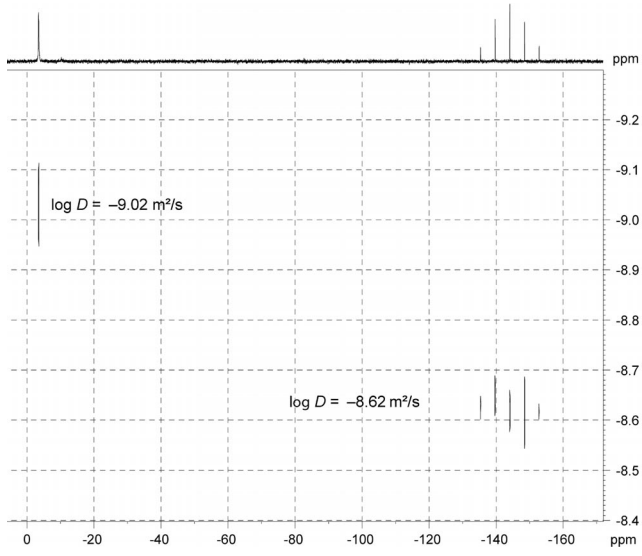

Figure 6. The ^{31}P DOSY NMR spectrum of complex **10**.

of a monomer. Moreover, the possibility that the dynamic process present in the dinuclear compound **3** might involve a fast dissociation step between the dinuclear and the mononuclear complexes, $[Cu_2\{(S,S)\text{-}i\text{Pr-pybox}\}_2(BnNC)_2][PF_6]_2$ and two $[Cu\{(S,S)\text{-}i\text{Pr-pybox}\}(CNBn)][PF_6]$, respectively, was also investigated. When comparing the results of several ^{1}H DOSY NMR spectroscopy experiments acquired with different diffusion times (diffusion time: 50, 100, 150, 250, and 500 ms),[23] the same diffusion coefficient (log *D* = –8.99 $m^2 s^{-1}$) was obtained for all the ^{1}H NMR spectroscopy resonances. This result supports the proposal that the structure of complex **3** is a stable, discrete, dinuclear molecule and rules out any possible exchange phenomenon between different molecular weight species. Moreover, the ^{1}H DOSY NMR spectrum was also recorded at 183 K and the resolved proton signals afforded a unique diffusion coefficient, which indicated the presence of only one diffusing molecule.

Conclusions

Studies of the reactivity of the $[Cu_2(R\text{-pybox})_2][X]_2$ complexes [R-pybox = (*S*,*S*)-*i*Pr-pybox (**1**) and (*R*,*R*)-Ph-pybox (**2**)] were reported in this paper. The results reflected that the dinuclear character of the precursor complexes was maintained upon reaction of **1** and **2** with the isocyanides (complexes **3**–**6**), while the mononuclear complexes (**7**–**9** and **13**–**14**) were formed upon reaction with the mononuclear ($PMePh_2$, PPh_3) and bidentate (dppf) phosphane ligands. On the other hand, the reaction of **1** and **2** with bidentate phosphanes with a similar bite angle, for example dppm and (*S*)-peap, gave rise to complexes of different nuclearity, namely $[Cu_2\{(S,S)\text{-}i\text{Pr-pybox}\}(\mu\text{-dppm})_2][PF_6]_2$ (**10**), $[Cu\{(S,S)\text{-}i\text{Pr-pybox}\}\{(S)\text{-peap}\}][PF_6]$ (**11**), and $[Cu\{(R,R)\text{-Ph-pybox}\}\{(S)\text{-peap}\}][PF_6]$ (**12**). The structure and size of the new mono- and dinuclear complexes, $[Cu_2\{(S,S)\text{-}i\text{Pr-pybox}\}_2(CNBn)_2][PF_6]_2$ (**3**), $[Cu\{(S,S)\text{-}i\text{Pr-pybox}\}(PMePh_2)_2][PF_6]$ (**7**), $[Cu_2\{(S,S)\text{-}i\text{Pr-pybox}\}(\mu\text{-dppm})_2][PF_6]_2$ (**10**), and $[Cu\{(S,S)\text{-}i\text{Pr-pybox}\}(dppf)][PF_6]$

(**13**), were determined both in the solid state and in the solution state through single-crystal X-ray analysis and NMR spectroscopy. The following conclusions arose from the ^{1}H, ^{19}F, and ^{31}P DOSY NMR spectroscopy studies: (i) the molecular size of the molecules present in solution was consistent with the molecular sizes found in the solid state and (ii) neither dissociated nor associated species were formed in the acetone solution. Additionally, no interaction between the ionic counterparts of the complexes was detected (NMR, [D$_6$]acetone). This work is likely to contribute to a better understanding of the coordination behavior of copper with respect to neutral Lewis bases. More importantly, it will be useful for designing new applications for copper catalysts with pybox-based ligands in organic synthesis.

Experimental Section

General Procedures: The reactions were performed under an atmosphere of dry nitrogen using a vacuum-line and the standard Schlenk technique. Solvents were dried by standard methods and distilled under a nitrogen atmosphere before use. [Cu_2(R-pybox)$_2$][PF_6]$_2$ [R-pybox = (*S*,*S*)-*i*Pr-pybox and (*R*,*R*)-Ph-pybox][5] and the phosphane ligands, bis(diphenylphosphanyl)methane (dppm),[24a] (–)-*N*,*N*-bis(diphenylphosphanyl)-(*S*)-1-phenylethylamine [(*S*)-peap],[24b] and 1,1′-bis(diphenylphosphanyl)ferrocene (dppf),[24c] were prepared by reported methods. The isocyanides and the monodentate phosphanes were obtained from commercial suppliers and used without further purification. Infrared spectra were recorded with a Perkin–Elmer 1720-XFT spectrometer. The conductivities were measured at room temperature in an acetone solution (ca. 5×10^{-4} M) with a Jenway PCM3 conductimeter. The C,H,N analyses were carried out with a Perkin–Elmer 240-B microanalyzer. Electrospray mass spectra (ESI-MS) were recorded with a MicroTof-Q Bruker instrument, which was operated in the positive mode and methanol was used as the solution. Mass spectra (MALDI-TOF) were determined with a Microflex Bruker spectrometer, which was operated in the positive mode, and dihydroxyanthranol was used as the matrix. Mass spectra (FAB) were recorded with a VG-AUTOSPEC mass spectrometer (positive mode) and 3-nitrobenzyl alcohol (NBA) was used as the matrix. The NMR spectra were recorded with Bruker spectrometers [AV600 operated at 600.15 (^{1}H) and 150.91 (^{13}C) MHz, AV400 operated at 400.13 (^{1}H), 100.61 (^{13}C), and 161.95 (^{31}P) MHz, or AV300 operated at 300.13 (^{1}H), 75.48 (^{13}C), 282.40 (^{19}F), and 121.49 (^{31}P) MHz]. DEPT experiments were carried out for all the compounds. 2D NMR spectra were recorded for selected complexes with Bruker AV400 and AV600 spectrometers. The chemical shifts are reported in ppm and referenced to TMS or 85% H_3PO_4 as the standards. The coupling constants *J* are given in Hertz (Hz). The following atom labels have been used for the ^{1}H and $^{13}C\{^{1}H\}$ NMR spectroscopic data of the pybox ligands.

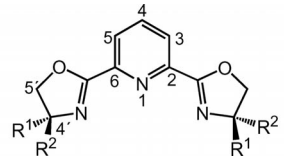

[Cu_2(R-pybox)$_2$(CNBn)$_2$][PF_6]$_2$ [R-pybox = (*S*,*S*)-*i*Pr-pybox (3), (*R*,*R*)-Ph-pybox (4)] and [Cu_2(R-pybox)$_2$(CNCy)$_2$][PF_6]$_2$ [R-pybox = (*S*,*S*)-*i*Pr-pybox (5), (*R*,*R*)-Ph-pybox (6)]: The isocyanide (CNBn or CNCy) (0.2 mmol) was added to a solution of [Cu_2(R-pybox)$_2$][PF_6]$_2$ (**1** or **2**) (0.1 mmol) in CH_2Cl_2 (10 mL). The resulting solution was stirred for 1 h. The solution was concentrated to ca. 2 mL and diethyl ether (30 mL) was added. The resulting yellow solid was washed with diethyl ether (3×10 mL) and dried under vacuum.

Complex 3: Yellow solid, yield 47% (0.059 g). Λ_M = 245 S cm^2 mol^{-1} (acetone, 293 K). IR (KBr): $\tilde{\nu}$ = (CN) 2184 (s), (PF_6^-) 841 (vs) cm^{-1}. MS-ESI (MeOH): *m*/*z* (%) = 481 (81) [Cu(*i*Pr-pybox)(CNBn)]$^+$, 364 (100) [Cu(*i*Pr-pybox)]$^+$, 297 (26) [Cu(CNBn)$_2$]$^+$. ^{1}H NMR (600.15 MHz, [D$_6$]acetone, 298 K): δ = 8.29 (br. s, 2 H, H^4 C_5H_3N), 7.95 (br. s, 4 H, H^{3,5} C_5H_3N), 7.44 (m, 10 H, Ph), 5.05 (m, 4 H, CNCH_2Ph), 4.88 (br. s, 4 H, OCH_2), 4.62 (br. s, 8 H, OCH_2, C*Hi*Pr), 2.20 (br. s, 4 H, C*H*Me$_2$), 1.08 (d, $J_{H,H}$ = 5.9 Hz, 12 H, CH*Me*$_2$), 1.05 (d, $J_{H,H}$ = 5.5 Hz, 12 H, CH*Me*$_2$) ppm. ^{1}H NMR (400.13 MHz, [D$_6$]acetone, 183 K): δ = 8.31 (t, $J_{H,H}$ = 7.8 Hz, 2 H, H^4 C_5H_3N), 7.85 (d, $J_{H,H}$ = 7.8 Hz, 2 H, H^{3,5} C_5H_3N), 7.52 (m, 10 H, Ph), 7.12 (d, $J_{H,H}$ = 7.8 Hz, 2 H, H^{3,5} C_5H_3N), 5.14 (s, 4 H, CNCH_2Ph), 5.10 (t, $J_{H,H}$ = 10.8 Hz, 2 H, OCH_2), 4.70–4.54 (m, 10 H, OCH_2, C*Hi*Pr), 2.43, 1.98 (2m, 2×2 H, C*H*Me$_2$), 1.00 (m, 24 H, CH*Me*$_2$) ppm. $^{13}C\{^{1}H\}$ NMR (150.91 MHz, [D$_6$]-acetone, 298 K): δ = 163.9 (s, O*C*N), 144.3 (s, C^{2,6} C_5H_3N), 140.2 (s, C^4 C_5H_3N), 139.0 (s, *C*NBn), 132.5 (s, C^{ipso} CNCH$_2$*Ph*), 129.1, 128.7, 127.4 (3s, Ph), 126.6 (s, C^{3,5} C_5H_3N), 72.5 (s, O*C*H$_2$), 71.6 (s, *C*H*i*Pr), 46.4 (s, CN*C*H$_2$Ph), 31.7 (s, *C*HMe$_2$), 17.7, 16.5 (2s, CH*Me*$_2$) ppm. $^{13}C\{^{1}H\}$ NMR (100.61 MHz, [D$_6$]acetone, 183 K): δ = 164.3, 163.5 (2s, O*C*N), 145.6, 141.9 (2s, C^{2,6} C_5H_3N), 140.3 (s, C^4 C_5H_3N), 137.2 (s, *C*NBn), 132.9 (s, C^{ipso} CNCH$_2$*Ph*), 129.3, 128.9, 127.5 (3s, Ph), 127.5, 125.7 (2s, C^{3,5} C_5H_3N), 74.5, 70.3 (2s, O*C*H$_2$), 72.2, 69.7 (2s, *C*H*i*Pr), 46.1 (s, CN*C*H$_2$Ph), 32.1, 30.1 (2s, *C*HMe$_2$), 18.1, 18.0, 17.5, 14.3 (4s, CH*Me*$_2$) ppm. $C_{50}H_{60}Cu_2F_{12}N_8O_4P_2$ (1254.08): calcd. C 47.89, H 4.82, N 8.94; found C 48.30, H 4.50, N 8.82.

Complex 5: Yellow solid, yield 55% (0.068 g). Λ_M = 200 S cm^2 mol^{-1} (acetone, 293 K). IR (KBr): $\tilde{\nu}$ = (CN) 2175 (m), (PF_6^-) 841 (vs) cm^{-1}. MS-MALDI-TOF: *m*/*z* (%) = 665 (100) [Cu(*i*Pr-pybox)$_2$]$^+$, 473 (56) [Cu(*i*Pr-pybox)(CNCy)]$^+$. ^{1}H NMR (400.13 MHz, [D$_6$]-acetone, 298 K): δ = 8.26 (m, 2 H, H^4 C_5H_3N), 7.89 (m, 4 H, H^{3,5} C_5H_3N), 5.00 (m, 4 H, OCH_2), 4.73 (m, 8 H, OCH_2, C*Hi*Pr), 4.05 (m, 2 H, H^1 CN*Cy*), 2.27 (m, 4 H, H^4 CN*Cy*), 1.98 (m, 4 H, C*H*Me$_2$), 1.71, 1.47 (2m, 2×8 H, H^{2,6}, H^{3,5} CN*Cy*), 1.13 (m, 24 H, CH*Me*$_2$) ppm. $^{13}C\{^{1}H\}$ NMR (100.61 MHz, [D$_6$]acetone, 298 K): δ = 164.1 (s, O*C*N), 144.3 (s, C^{2,6} C_5H_3N), 140.1 (s, C^4 C_5H_3N), 136.9 (s, *C*NCy), 126.6 (s, C^{3,5} C_5H_3N), 72.7 (s, O*C*H$_2$), 71.4 (s, *C*H*i*Pr), 53.1 (s, C^1 CN*Cy*), 31.8 (s, *C*HMe$_2$), 31.7 (s, C^4 CN*Cy*), 24.5, 22.4 (2s, C^{2,6}, C^{3,5} CN*Cy*), 17.6, 16.5 (2s, CH*Me*$_2$) ppm. $C_{48}H_{68}Cu_2F_{12}N_8O_4P_2$·$CH_2Cl_2$ (1323.06): calcd. C 44.48, H 5.33, N 8.47; found C 44.22, H 5.20, N 8.25.

Complex 6: Yellow solid, yield 60% (0.082 g). Λ_M = 177 S cm^2 mol^{-1} (acetone, 293 K). IR (KBr): $\tilde{\nu}$ = (CN) 2178 (s), (PF_6^-) 840 (vs) cm^{-1}. MS-MALDI-TOF: *m*/*z* (%) = 801 (100) [Cu(Ph-pybox)$_2$]$^+$, 541 (27) [Cu(Ph-pybox)(CNCy)]$^+$. ^{1}H NMR (300.13 MHz, [D$_6$]acetone, 298 K): δ = 8.48 (m, 2 H, H^4 C_5H_3N), 8.41 (m, 4 H, H^{3,5} C_5H_3N), 7.44–7.36 (m, 20 H, Ph), 5.82, 5.36, 4.70 (3m, 3×4 H, OCH_2, C*H*Ph), 3.78 (m, 2 H, H^1 CN*Cy*), 1.76 (m, 4 H, H^4 CN*Cy*), 1.49, 1.33 (2m, 2×8 H, H^{2,6}, H^{3,5} CN*Cy*) ppm. $^{13}C\{^{1}H\}$ NMR (100.61 MHz, [D$_6$]acetone, 298 K): δ = 164.9 (s, O*C*N), 144.6 (s, C^{2,6} C_5H_3N), 140.5 (s, C^4 C_5H_3N), 140.1 (s, *C*NCy), 128.7, 128.3, 127.2 (3s, Ph, C^{3,5} C_5H_3N), 77.5 (s, OCH$_2$), 69.3 (s, *C*HPh), 52.9 (s, C^1 CN*Cy*), 31.5 (s, C^4 CN*Cy*), 24.4, 22.3 (2s, C^{2,6}, C^{3,5} CN*Cy*) ppm. $C_{60}H_{60}Cu_2F_{12}N_8O_4P_2$·$CH_2Cl_2$ (1459.12): calcd. C 50.21, H 4.28, N 7.68; found C 50.02, H 4.00, N 7.74.

[Cu(R-pybox)(PRPh$_2$)$_2$][PF$_6$] [R-pybox = (*S*,*S*)-*i*Pr-pybox, R = Me (7), Ph (8); R-pybox = (*R*,*R*)-Ph-pybox, R = Ph (9)]: The phosphane ($PMePh_2$ or PPh_3) (0.4 mmol) was added to a solution of [Cu$_2$(R-pybox)$_2$][PF$_6$]$_2$ (**1** or **2**) (0.1 mmol) in CH_2Cl_2 (10 mL). The resulting solution was stirred for 1 h. The solution was concentrated to ca. 2 mL and diethyl ether (30 mL) (for **8** and **9**) or a mixture of diethyl ether/hexane (2:1, 30 mL) (for **7**) was added. The resulting solid was washed with diethyl ether/hexane (2:1, 3 × 10 mL) and dried under vacuum.

Complex 7: Yellow solid, yield 75% (0.068 g). Λ_M = 137 S cm^2 mol^{-1} (acetone, 293 K). IR (KBr): $\tilde{\nu}$ = (PF_6^-) 840 (vs) cm^{-1}. MS-FAB: *m*/*z* (%) = 564 (21) [Cu(*i*Pr-pybox)($PMePh_2$)]$^+$, 364 (100) [Cu(*i*Pr-pybox)]$^+$. $^{31}P\{^1H\}$ NMR (121.49 MHz, [D$_6$]acetone, 298 K): δ = –17.1 (br. s) ppm. ^1H NMR (600.15 MHz, [D$_6$]acetone, 298 K): δ = 8.35 (t, $J_{H,H}$ = 7.7 Hz, 1 H, H^4 C_5H_3N), 8.25 (d, $J_{H,H}$ = 7.7 Hz, 2 H, H^{3,5} C_5H_3N), 7.54 (t, $J_{H,H}$ = 7.1 Hz, 4 H, Ph), 7.48 (d, $J_{H,H}$ = 7.1 Hz, 2 H, Ph), 7.42 (m, 6 H, Ph), 7.37 (m, 8 H, Ph), 4.34 (m, 2 H, OC*H*$_2$) 4.21 (t, $J_{H,H}$ = 8.2 Hz, 2 H, OC*H*$_2$), 3.91 (m, 2 H, C*H*i*Pr*), 1.96 (s, 6 H, P*Me*Ph$_2$), 1.54 (m, 2 H, C*H*Me$_2$), 0.75 (d, $J_{H,H}$ = 6.5 Hz, 6 H, CH*Me*$_2$), 0.57 (d, $J_{H,H}$ = 5.5 Hz, 6 H, CH*Me*$_2$) ppm. $^{13}C\{^1H\}$ NMR (150.91 MHz, [D$_6$]acetone, 298 K): δ = 162.0 (s, O*C*N), 145.1 (s, C^{2,6} C_5H_3N), 139.9 (s, C^4 C_5H_3N), 135.7, 134.7 (2s, C^{ipso} Ph), 132.2, 131.4, 130.0, 129.5, 128.8, 128.7 (6s, Ph), 127.4 (s, C^{3,5} C_5H_3N), 71.3 (s, *C*H*i*Pr), 70.6 (s, O*C*H$_2$), 31.0 (s, *C*HMe$_2$), 18.4, 15.5 (2s, CH*Me*$_2$), 12.1 (s, P*Me*Ph$_2$) ppm. $C_{43}H_{49}CuF_6N_3O_2P_3$ (910.33): calcd. C 56.73, H 5.43, N 4.62; found C 56.66, H 5.16, N 4.47.

Complex 9: Yellow solid, yield 76% (0.084 g). Λ_M = 107 S cm^2 mol^{-1} (acetone, 293 K). IR (KBr): $\tilde{\nu}$ = (PF_6^-) 839 (vs) cm^{-1}. MS-FAB: *m*/*z* (%) = 694 (22) [Cu(Ph-pybox)(PPh_3)]$^+$, 587 (21) [Cu(PPh_3)$_2$]$^+$, 432 (100) [Cu(Ph-pybox)]$^+$, 325 (39) [Cu(PPh_3)]$^+$. $^{31}P\{^1H\}$ NMR (121.49 MHz, [D$_6$]acetone, 298 K): δ = 2.01 (br. s) ppm. ^1H NMR (300.13 MHz, [D$_6$]acetone, 298 K): δ = 8.49–8.44 (m, 3 H, H^{3,4,5} C_5H_3N), 7.45–6.96 (m, 40 H, Ph), 4.96, 4.54, 4.06 (3m, 3 × 2 H, OC*H*$_2$, C*H*Ph) ppm. $^{13}C\{^1H\}$ NMR (100.61 MHz, [D$_6$]acetone, 298 K): δ = 164.7 (s, O*C*N), 146.3 (s, C^{2,6} C_5H_3N), 141.7 (s, C^4 C_5H_3N), 133.5–126.7 (16s, Ph, C^{3,5} C_5H_3N), 77.8 (s, O*C*H$_2$), 70.1 (s, *C*HPh) ppm. $C_{59}H_{49}CuF_6N_3O_2P_3$ (1102.50): calcd. C 64.28, H 4.48, N 3.81; found C 64.37, H 4.64, N 3.90.

[Cu$_2${(*S*,*S*)-*i*Pr-pybox}(μ-dppm)$_2$][PF$_6$]$_2$ (10): Dppm (0.4 mmol, 0.154 g) was added to a solution of complex **1** (0.2 mmol) in CH_2Cl_2 (10 mL). The resulting solution was stirred for 3 h. The solution was concentrated to ca. 2 mL and diethyl ether (30 mL) was added. The resulting yellow solid was washed with diethyl ether/hexane (2:1, 3 × 10 mL) and dried under vacuum. Cream solid, yield 67% (0.100 g). Λ_M = 203 S cm^2 mol^{-1} (acetone, 293 K). IR (KBr): $\tilde{\nu}$ = (PF_6^-) 840 (vs) cm^{-1}. MS-FAB: *m*/*z* (%) = 831 (11) [Cu(dppm)$_2$]$^+$, 748 (12) [Cu(*i*Pr-pybox)(dppm)]$^+$, 665 (14) [Cu(*i*Pr-pybox)$_2$]$^+$, 447 (49) [Cu(dppm)]$^+$, 364 (100) [Cu(*i*Pr-pybox)]$^+$. $^{31}P\{^1H\}$ NMR (121.49 MHz, [D$_6$]acetone, 298 K): δ = –3.6 (br. s) ppm. ^1H NMR (600.15 MHz, [D$_6$]acetone, 298 K): δ = 8.71 (t, $J_{H,H}$ = 8.0 Hz, 1 H, H^4 C_5H_3N), 8.50 (d, $J_{H,H}$ = 8.0 Hz, 2 H, H^{3,5} C_5H_3N), 7.58 (m, 12 H, Ph), 7.48 (t, $J_{H,H}$ = 7.4 Hz, 4 H, Ph), 7.33 (m, 16 H, Ph), 7.11 (br. s, 8 H, Ph), 4.52 (dd, $J_{H,H}$ = 7.9, 4.8 Hz, 2 H, OC*H*$_2$), 3.94 [m, 8 H, C*H*i*Pr*, OC*H*$_2$, C*H*$_2$(PPh$_2$)$_2$], 1.54 (m, 2 H, C*H*Me$_2$), 0.70 (d, $J_{H,H}$ = 6.7 Hz, 6 H, CH*Me*$_2$), 0.49 (d, $J_{H,H}$ = 7.0 Hz, 6 H, CH*Me*$_2$) ppm. $^{13}C\{^1H\}$ NMR (150.91 MHz, [D$_6$]acetone, 298 K): δ = 164.9 (s, O*C*N), 145.7 (s, C^{2,6} C_5H_3N), 142.1 (s, C^4 C_5H_3N), 133.3 (s, Ph), 132.6 (m, C^{ipso} Ph), 131.9, 131.4 (2s, Ph), 131.0 (m, C^{ipso} Ph), 130.8 (s, Ph), 130.2 (s, C^{3,5} C_5H_3N), 129.5, 129.3 (2s, Ph), 71.5 (s, *C*H*i*Pr), 69.1 (s, O*C*H$_2$), 30.9 (s, *C*HMe$_2$), 26.3 (s, *C*H$_2$(PPh$_2$)$_2$), 18.1, 13.9 (2s, CH*Me*$_2$) ppm. $C_{67}H_{67}Cu_2F_{12}N_3O_2P_6$ (1487.18): calcd. C 54.11, H 4.54, N 2.83; found C 54.01, H 4.54, N 3.00.

[Cu(R-pybox){(*S*)-peap}][PF$_6$] [R-pybox = (*S*,*S*)-*i*Pr-pybox (11), (*R*,*R*)-Ph-pybox (12)] and [Cu(R-pybox)(dppf)][PF$_6$] [R-pybox = (*S*,*S*)-*i*Pr-pybox (13), (*R*,*R*)-Ph-pybox (14)]: (*S*)-Peap or dppf (0.2 mmol) was added to a solution of complex **1** or **2** (0.1 mmol) in CH_2Cl_2 (15 mL). The resulting solution was stirred for 1 h (for **11** and **12**) or 3 h (for **13** and **14**). The solution was concentrated to ca. 2 mL and a mixture of diethyl ether/hexane (2:1, 30 mL) was added. The resulting yellow solid was washed with diethyl ether/hexane (2:1, 3 × 30 mL) and dried under vacuum.

Complex 11: Yellow solid, yield 52% (0.052 g). Λ_M = 103 S cm^2 mol^{-1} (acetone, 293 K). IR (KBr): $\tilde{\nu}$ = (PF_6^-) 840 (vs) cm^{-1}. MS-ESI (MeOH): *m*/*z* (%) = 1041 (100) [Cu{(*S*)-peap)}$_2$]$^+$, 665 (13) [Cu(*i*Pr-pybox)$_2$]$^+$. $^{31}P\{^1H\}$ NMR (161.95 MHz, [D$_6$]acetone, 298 K): δ = 88.2 (br. s) ppm. ^1H NMR (400.13 MHz, [D$_6$]acetone, 298 K): δ = 8.37 (m, 3 H, H^{3,4,5} C_5H_3N), 7.62–7.32 (m, 20 H, PPh_2), 6.93 (t, $J_{H,H}$ = 7.3 Hz, 1 H, H^4 NCHMe*Ph*), 6.82 (t, $J_{H,H}$ = 7.3 Hz, 2 H, H^{3,5} NCHMe*Ph*), 6.59 (d, $J_{H,H}$ = 7.3 Hz, 2 H, H^{2,6} NCHMe*Ph*), 4.80 (d, $J_{H,H}$ = 7.1 Hz, 1 H, NC*H*MePh), 4.66, 4.21 (2m, 2 × 2 H, OC*H*$_2$), 4.06 (m, 2 H, C*H*i*Pr*), 1.71 (m, 2 H, C*H*Me$_2$), 0.96 (d, $J_{H,H}$ = 7.1 Hz, 3 H, NCH*Me*Ph), 0.86, 0.80 (2d, $J_{H,H}$ = 6.2 Hz, 2 × 6 H, CH*Me*$_2$) ppm. $^{13}C\{^1H\}$ NMR (100.61 MHz, [D$_6$]acetone, 298 K): δ = 164.0 (s, O*C*N), 145.3 (s, C^{2,6} C_5H_3N), 141.3 (s, C^{ipso} Ph), 133.8, 133.3, 132.3, 131.8, 129.8, 129.1, 128.8, 128.5 (8s, Ph, C^{3,4,5} C_5H_3N), 73.6 (s, O*C*H$_2$), 72.5 (s, *C*H*i*Pr), 62.1 (s, N*C*HMePh), 33.0 (s, *C*HMe$_2$), 29.3 (s, CH*Me*$_2$), 22.1 (s, NCH*Me*Ph) ppm. $C_{49}H_{52}CuF_6N_4O_2P_3{\cdot}CH_2Cl_2$ (1084.35): calcd. C 55.38, H 5.02, N 5.17; found C 56.07, H 4.90, N 5.20.

Complex 12: Yellow solid, yield 48% (0.052 g). Λ_M = 94 S cm^2 mol^{-1} (acetone, 293 K). IR (KBr): $\tilde{\nu}$ = (PF_6^-) 839 (vs) cm^{-1}. MS-ESI (MeOH): *m*/*z* (%) = 1041 (100) [Cu{(*S*)-peap}$_2$]$^+$, 801 (9) [Cu(Ph-pybox)$_2$]$^+$. $^{31}P\{^1H\}$ NMR (121.49 MHz, [D$_6$]acetone, 298 K): δ = 88.9 (br. s) ppm. ^1H NMR (300.13 MHz, [D$_6$]acetone, 298 K): δ = 8.22 (m, 3 H, H^{3,4,5} C_5H_3N), 7.45–7.20 (m, 30 H, Ph), 6.24 (t, $J_{H,H}$ = 7.3 Hz, 1 H, H^4 NCHMe*Ph*), 6.82 (t, $J_{H,H}$ = 7.3 Hz, 2 H, H^{3,5} NCHMe*Ph*), 6.58 (d, $J_{H,H}$ = 7.3 Hz, 2 H, H^{2,6} NCHMe*Ph*), 5.43, 5.02, 4.29 (3m, 3 × 2 H, C*H*Ph, OC*H*$_2$), 4.80 (m, 1 H, NC*H*MePh), 0.96 (d, $J_{H,H}$ = 7.2 Hz, 3 H, NCH*Me*Ph) ppm. $^{13}C\{^1H\}$ NMR (100.61 MHz, [D$_6$]acetone, 298 K): δ = 165.0 (s, O*C*N), 140.4 (s, C^{2,6} C_5H_3N), 139.5, 139.3 (2s, C^{ipso} Ph), 132.9, 132.4, 131.9, 131.3, 130.9, 129.0, 128.9, 128.6, 128.2, 127.9, 127.6, 126.7 (12s, Ph, C^{3,4,5} C_5H_3N), 76.5 (s, O*C*H$_2$), 69.1 (s, *C*HPh), 61.2 (s, N*C*HMePh), 21.2 (s, NCH*Me*Ph) ppm. $C_{55}H_{48}CuF_6N_4O_2P_3{\cdot}CH_2Cl_2$ (1152.39): calcd. C 58.37, H 4.37, N 4.86; found C 58.63, H 4.10, N 4.92.

Complex 13: Yellow solid, yield 95% (0.101 g). Λ_M = 137 S cm^2 mol^{-1} (acetone, 293 K). IR (KBr): $\tilde{\nu}$ = (PF_6^-) 843 (vs) cm^{-1}. MS-ESI (MeOH): *m*/*z* (%) = 918 (87) [Cu(*i*Pr-pybox)(dppf)]$^+$, 665 (85) [Cu(*i*Pr-pybox)$_2$]$^+$, 617 (100) [Cu(dppf)]$^+$, 364 (77) [Cu(*i*Pr-pybox)]$^+$. $^{31}P\{^1H\}$ NMR (161.95 MHz, [D$_6$]acetone, 298 K): δ = –12.1 (br. s) ppm. ^1H NMR (600.15 MHz, [D$_6$]acetone, 298 K): δ = 8.43 (s, 3 H, H^{3,4,5} C_5H_3N), 7.77 (br. s, 4 H, Ph), 7.45 (m, 12 H, Ph), 7.24 (br. s, 4 H, Ph), 5.08, 4.80, 4.64, 4.18 (4s, 4 × 2 H, Cp), 4.00 (m, 2 H, OC*H*$_2$), 3.95 (t, $J_{H,H}$ = 9.2 Hz, 2 H, OC*H*$_2$), 3.68 (m, 2 H, C*H*i*Pr*), 1.62 (m, 2 H, C*H*Me$_2$), 0.78 (d, $J_{H,H}$ = 7.0 Hz, 6 H, CH*Me*$_2$), 0.62 (d, $J_{H,H}$ = 6.7 Hz, 6 H, CH*Me*$_2$) ppm. $^{13}C\{^1H\}$ NMR (150.91 MHz, [D$_6$]acetone, 298 K): δ = 162.2 (s, O*C*N), 146.0 (s, C^{2,6} C_5H_3N), 140.1 (s, C^4 C_5H_3N), 135.9 (s, C^{ipso} Ph), 134.0 (t, $J_{C,P}$ = 7.4 Hz, C^{2,6} Ph), 132.9 (t, J_{CP} = 17.1 Hz, C^{ipso} Ph), 131.9 (br. s, C^{2,6} Ph), 130.4 (s, C^4 Ph), 129.6 (s, C^4 Ph), 128.8 (s, C^{3,5} Ph), 128.7 (t, $J_{C,P}$ = 5.1 Hz, C^{3,5} Ph), 128.0 (s, C^{3,5} C_5H_3N), 76.4 (t, $J_{C,P}$ = 11.0 Hz, Cp), 74.1 (s, Cp), 73.7 (s, Cp), 72.1 (d, $J_{C,P}$ = 98 Hz,

C^{ipso} Cp), 71.3 (s, Cp), 71.0 (s, *C*H*i*Pr), 70.2 (s, O*C*H$_2$), 30.8 (s, *C*HMe$_2$), 18.3, 15.1 (2s, CH*Me*$_2$) ppm.

Complex 14: Yellow solid, yield 62% (0.070 g). Λ_M = 132 S cm^2 mol^{-1} (acetone, 293 K). IR (KBr): $\tilde{\nu}$ = (PF_6^-) 840 (vs) cm^{-1}. MS-FAB: *m*/*z* (%) = 986 (100) [Cu(Ph-pybox)(dppf)]$^+$, 617 (15) [Cu(dppf)]$^+$. $^{31}P\{^1H\}$ NMR (161.95 MHz, [D$_6$]acetone, 298 K): δ = –12.4 (br. s) ppm. ^1H NMR (400.13 MHz, [D$_6$]acetone, 298 K): δ = 8.54 (m, 2 H, H^{3,5} C_5H_3N), 8.22 (m, 1 H, H^4 C_5H_3N), 7.48–6.91 (m, 30 H, Ph), 4.94 (m, 2 H, Cp), 4.58 (t, $J_{H,H}$ = 8.3 Hz, 2 H, OC*H*$_2$), 4.40, 4.19 (2m, 2 × 4 H, C*H*Ph, OC*H*$_2$, Cp), 3.97 (m, 2 H, Cp) ppm. $^{13}C\{^1H\}$ NMR (100.61 MHz, [D$_6$]acetone, 298 K): δ = 163.8 (s, O*C*N), 146.2 (s, C^{2,6} C_5H_3N), 141.1, 140.5 (2s, C^{ipso} Ph), 134.8 (s, C^4 C_5H_3N), 131.4, 130.1, 129.5, 129.0, 128.6, 128.3, 127.1 (7s, Ph, C^{3,5} C_5H_3N), 77.0 (s, O*C*H$_2$), 76.0 (s, C^{ipso} Cp), 74.2, 73.7, 71.1 (3s, Cp), 69.7 (s, *C*HPh) ppm. $C_{57}H_{47}CuF_6FeN_3O_2P_3$·1/2 CH_2Cl_2 (1174.77): calcd. C 58.79, H 4.12, N 3.58; found C 58.63, H 4.66, N 3.70.

X-ray Data: Suitable crystals for X-ray diffraction analysis were obtained by diffusion of diethyl ether (**3** and **10**) and hexane (**7** and **13**) into a solution of the complexes in dichloromethane. The unit cell of complex **10** contains dichloromethane and diethyl ether (1:2:1). The most relevant crystal and refinement data collected are in Table 3.

The data collection was performed with a Nonius Kappa CCD single-crystal diffractometer with Cu-K_α radiation (λ = 1.5418 Å) (for **3** and **10**) and Mo-K_α radiation (λ = 0.71073 Å) (for **13**). The images were collected at a 30 mm fixed crystal-detector distance by the oscillation method with 1° oscillation and 60 s exposure time per image. The data collection strategy was calculated with the program Collect.[25] The data reduction and the cell refinement were performed with the programs HKL Denzo and Scalepack.[26] A semi-empirical absorption correction was applied using the program SORTAV.[27]

Data collection for **7** was performed with an Oxford Diffraction Xcalibur Gemini S single-crystal diffractometer with Mo-K_α radiation (λ = 0.71073 Å). The images were collected at a 45 mm fixed crystal-detector distance by the oscillation method with 1° oscillation and 100 s exposure time per image. The data collection strategy was calculated with the program CrysAlis Pro CCD.[28] The data reduction and the cell refinement were performed with the program CrysAlis Pro RED.[28] An empirical absorption correction was applied using the SCALE3 ABSPACK algorithm as implemented in the program CrysAlis Pro RED.[28]

In all cases, the software package WINGX[29] was used for space group determination, structure solution, and refinement. The structures were solved by Patterson interpretation and phase expansion using DIRDIF.[30] Isotropic least-squares refinement on F^2 using SHELXL97[31] was performed. During the final stages of the refinements, all the positional parameters and the anisotropic temperature factors of all the non-H atoms were refined. The H atoms were geometrically located and their coordinates were refined riding on their parent atoms. The function that was minimized was $([\Sigma w(F_o^2 - F_c^2)/\Sigma w(F_o^2)]^{1/2}$ where $w = 1/[\sigma^2(F_o^2) + (aP)^2 + bP]$ (the *a* and *b* values are in Table 3), with $\sigma(F_o^2)$ from counting statistics and $P = (\max(F_o^2,0) + 2F_c^2)/3$. The atomic scattering factors were taken from the International Tables for X-ray Crystallography.[32] The geometrical calculations were made with PARST.[33] The crystallographic plots were made with PLATON.[34]

Table 3. The crystal data and structure refinement for complexes **3**, **7**, **10**·2CH_2Cl_2·Et_2O, and **13**.

	3	**7**	**10**·2CH_2Cl_2·Et_2O	**13**
Empirical formula	$C_{50}H_{60}Cu_2F_{12}N_8O_4P_2$	$C_{43}H_{49}CuF_6N_3O_2P_3$	$C_{73}H_{81}Cl_4Cu_2F_{12}N_3O_3P_6$	$C_{51}H_{51}CuF_6FeN_3O_2P_3$
Fw	1254.08	910.30	1731.11	1064.25
T [K]	293(2)	293(2)	150(2)	293(2)
wavelength [Å]	1.5418	0.71073	1.5418	0.71073
Crystal system	orthorhombic	orthorhombic	monoclinic	monoclinic
Space group	$P2_12_12_1$	$P2_12_12_1$	$P2_1$	$P2_1$
a [Å]	10.6609(1)	10.2381(4)	13.4328(2)	11.5737(3)
b [Å]	12.4172(1)	11.5699(5)	23.1484(2)	14.1437(3)
c [Å]	44.4579(5)	37.6037(15)	13.9496(1)	14.8633(3)
β [°]	90	90	116.066(1)	98.205(1)
V [Å^3]	5885.27(10)	4454.3(3)	3896.41(7)	2408.14(9)
Z	4	4	2	2
ρ_{calcd} [Mg m^{-3}]	1.415	1.357	1.475	1.468
μ [mm^{-1}]	2.162	0.662	3.757	0.910
F (000)	2576	1888	1776	1096
Crystal size [mm^3]	0.30 × 0.25 × 0.25	0.07 × 0.12 × 0.24	0.40 × 0.30 × 0.10	0.32 × 0.07 × 0.07
θ range [°]	3.98 to 68.16	2.17 to 32.63	3.66 to 68.49	2.00 to 25.51
Index ranges (*h*,*k*,*l*)	(0/12), (0/14), ±53	(–13/14), ±16, ±55	(–16/14), (–27/21), (0/16)	(–14/13), ±17, (0/17)
Reflections collected	19314	34606	27247	33212
Independent reflections (R_{int})	10078 (0.032)	13875 (0.0722)	11842 (0.0451)	8899 (0.057)
Completeness to θ_{max} [%]	95.4	92.7	98.5	99.3
Refinement method	full-matrix least-squares on F^2			
Number of parameters / restraints	711 / 0	529 / 0	928 / 1	608 / 0
GOF on F^2	1.037	0.764	1.139	1.009
Weight function (a,b)	0.1009, 0.6798	0.0471, 0.000	0.0885, 8.4269	0.0638, 0.000
R_1 / wR_2 [$I > 2\sigma(I)$][a]	0.0519 / 0.1452	0.0492 / 0.0945	0.0535 / 0.1471	0.0450 / 0.1267
R_1 / wR_2 (all data)	0.0659 / 0.1572	0.1734 / 0.1145	0.0617 / 0.1780	0.0591 / 0.1380
Absolute structure parameters	–0.01(3)	0.006(12)	0.03(2)	–0.009(16)
Largest diff. peak [e Å^{-3}]	0.407	0.634	0.950	0.451
Largest diff. hole [e Å^{-3}]	–0.347	–0.238	–0.964	–0.809

[a] $R_1 = \Sigma(|F_o| - |F_c|)/\Sigma|F_o|$; $wR_2 = \{\Sigma[w(F_o^2 - F_c^2)^2]/\Sigma[w(F_o^2)^2]\}^{1/2}$.

Supporting Information (see also the footnote on the first page of this article): Full characterization of complexes **4** and **8,** as well as the synthesis and characterization of complexes **3a**–**4a** and **7a**–**9a,** the experimental conditions for the NMR spectroscopic experiments, and the 1D, 2D, and variable-temperature NMR spectroscopy for complexes **3**, **7**, **10**, and **13**.

CCDC-791817 (for **3**), -791818 (for **7**), -791819 (for **10**·$2CH_2Cl_2$·Et_2O), and -791820 (for **13**) contain the supplementary crystallographic data for this paper. These data can be obtained free of charge from The Cambridge Crystallographic Data Centre via www.ccdc.cam.ac.uk/data_request/cif.

Acknowledgments

This work was supported by the Spanish Ministerio de Educación y Ciencia (MEC) (CTQ2006-08485) and Consolider Ingenio 2010 (CSD2007-00006).

[1] a) A. Datta Gupta, D. Bhuniya, V. K. Singh, *Tetrahedron* **1994**, *50*, 13725–13730; b) P. Müller, C. Boléa, *Helv. Chim. Acta* **2001**, *84*, 1093–1111; c) P. Müller, C. Boléa, *Synlett* **2000**, 826–828.

[2] S. K. Ginotra, V. K. Singh, *Tetrahedron* **2006**, *62*, 3573–3581, and references cited therein.

[3] J.-C. Meng, V. V. Fokin, M. G. Finn, *Tetrahedron Lett.* **2005**, *46*, 4543–4546.

[4] a) C. Wei, C. J. Li, *J. Am. Chem. Soc.* **2002**, *124*, 5638–5639; b) C. Wei, J. T. Mague, C. J. Li, *Proc. Natl. Acad. Sci. USA* **2004**, *101*, 5749–5754; c) A. Bisai, V. K. Singh, *Org. Lett.* **2006**, *8*, 2405–2408.

[5] M. Panera, J. Díez, I. Merino, E. Rubio, M. P. Gamasa, *Inorg. Chem.* **2009**, *48*, 11147–11160.

[6] W. J. Geary, *Coord. Chem. Rev.* **1971**, *7*, 81–122.

[7] a) J. Díez, M. P. Gamasa, J. Gimeno, M. Lanfranchi, A. Tiripicchio, *J. Organomet. Chem.* **2001**, *637–639*, 677–682; b) W. Imhof, K. Halbauer, H. Görls, *Acta Crystallogr., Sect. E.* **2005**, *61*, 1995–1997; c) H. V. R. Dias, G. G. Lobbia, G. Papini, M. Pellei, C. Santini, *Eur. J. Inorg. Chem.* **2009**, *26*, 3935–3941.

[8] a) G. A. Bowmaker, J. V. Hanna, F. E. Hahn, A. S. Lipton, C. E. Oldham, B. W. Skelton, M. E. Smith, A. H. White, *Dalton Trans.* **2008**, 1710–1720; b) H. V. R. Dias, H. L. Lu, J. D. Gorden, W. C. Jin, *Inorg. Chem.* **1996**, *35*, 2149–2151; c) T. Bartolomas, D. Lentz, I. Neubert, M. Rottger, *Z. Anorg. Allg. Chem.* **2002**, *628*, 863–871.

[9] a) X. Gan, W.-F. Fu, Y.-Y. Lin, M. Yuan, C.-M. Che, S.-M. Chi, H.-F. J. Li, J.-H. Chen, Y. Chen, Z.-Y. Zhou, *Polyhedron* **2008**, *27*, 2202–2208; b) D. Li, R.-Z. Li, Z. Ni, Z.-Y. Qi, X.-L. Feng, J.-W. Cai, *Inorg. Chem. Commun.* **2003**, *6*, 469–473.

[10] a) R. J. Puddephatt, *Chem. Soc. Rev.* **1983**, *12*, 99–127; b) B. Chaudret, B. Delavaux, R. Poilblanc, *Coord. Chem. Rev.* **1988**, *86*, 191–243; c) G. K. Anderson, *Adv. Organomet. Chem.* **1993**, *35*, 1–39.

[11] For representative examples of dinuclear bridging dppm-copper(I) complexes, see: a) J. Díez, M. P. Gamasa, J. Gimeno, A. Tiripicchio, M. T. Camellini, *J. Chem. Soc., Dalton Trans.* **1987**, 1275–1278; b) J. Díez, M. P. Gamasa, J. Gimeno, M. Lanfranchi, A. Tiripicchio, *J. Chem. Soc., Dalton Trans.* **1990**, 1027–1033; c) W.-W. Yam, V. C.-H. Lam, K.-K. Cheung, *Chem. Commun.* **2001**, 545–546; d) Y. Chen, J.-S. Chen, X. Gan, W.-F. Fu, *Inorg. Chim. Acta* **2009**, *362*, 2492–2498.

[12] To the best of our knowledge, copper(I) complexes with diphosphazane ligands have not been reported. Representative non-copper complexes with diphosphazane bridging ligands: a) H. Krishna, S. S. Krishnamurthy, M. Nethaji, *Polyhedron* **2006**, *25*, 3189–3200; b) V. S. Reddy, S. S. Krishnamurthy, M. Nethaji, *J. Chem. Soc., Dalton Trans.* **1995**, 1933–1938; c) S. K. Mandal, T. S. Venkatakrishnan, A. Sarkar, S. S. Krishnamurthy, *J. Organomet. Chem.* **2006**, *691*, 2969–2977; d) E. J. Sekabunga, M. L. Smith, T. R. Webb, W. E. Hill, *Inorg. Chem.* **2002**, *41*, 1205–1214.

[13] a) J. Díez, M. P. Gamasa, J. Gimeno, A. Aguirre, S. García-Granda, J. Holubova, L. R. Falvello, *Organometallics* **1999**, *18*, 662–669, and references cited therein; b) G. Bandoli, A. Dolmella, *Coord. Chem. Rev.* **2000**, *209*, 161–196; c) N. Begum, U. K. Das, M. Hassan, G. Hogarth, S. E. Kabir, E. Nordlander, M. A. Rahman, D. A. Tocher, *Organometallics* **2007**, *26*, 6462–6472.

[14] a) F. A. Cotton, X. Feng, M. Matusz, R. Poli, *J. Am. Chem. Soc.* **1988**, *110*, 7077–7083; b) F. A. Cotton, X. Feng, D. J. Timmons, *Inorg. Chem.* **1998**, *37*, 4066–4069.

[15] a) G. Pilloni, B. Longato, G. Bandoli, *Inorg. Chim. Acta* **1998**, *277*, 163–170; b) S. P. Neo, Z.-Y. Zhou, T. C. W. Mak, T. S. A. Hor, *J. Chem. Soc., Dalton Trans.* **1994**, 3451–3458.

[16] A. Bondi, *J. Phys. Chem.* **1964**, *68*, 441–451; the van der Waals radius of iron is 2.0 Å according to the CSD base data.

[17] a) K. F. Morris, C. S. Johnson Jr., *J. Am. Chem. Soc.* **1992**, *114*, 3139–3141; b) C. S. Johnson Jr., *Prog. Nucl. Magn. Reson. Spectrosc.* **1999**, *34*, 203–256; c) D. W. Timothy Claridge, *High Resolution NMR Techniques in Organic Chemistry*, in: *Tetrahedron Organic Chemistry Series*, 2nd edition, Elsevier Ed., Oxford, **2009**, chapter 9.

[18] For some selected examples, see: a) S. Viel, L. Mannina, A. Segre, *Tetrahedron Lett.* **2002**, *43*, 2515–2519; b) M. D. Díaz, S. Berger, *Carbohydr. Res.* **2000**, *329*, 1–5; c) I. Keresztes, P. G. Williard, *J. Am. Chem. Soc.* **2000**, *122*, 10228–10229; d) X. Ribas, J. C. Dias, J. Morgado, K. Wurst, M. Almeida, T. Parella, J. Veciana, C. Rovira, *Angew. Chem. Int. Ed.* **2004**, *43*, 4049–4052; e) N. Schlörer, E. J. Cabrita, S. Berger, *Angew. Chem. Int. Ed.* **2002**, *41*, 107–109.

[19] Stokes–Einstein equation: $D = K_BT/6\pi\eta r_H$, (D = diffusion coefficient, K_B = Boltzmann constant, η = solvent viscosity, r_H = hydrodynamic radius).

[20] a) M. Valentini, P. S. Pregosin, H. Rüegger, *Organometallics* **2000**, *19*, 2551–2555; b) J. D. Hoefelmeyer, D. L. Brode, F. P. Gabbai, *Organometallics* **2001**, *20*, 5653–5657.

[21] N. Esturau, F. Sánchez-Ferrando, J. A. Gavín, C. Roumestand, M.-A. Delsuc, T. Parella, *J. Magn. Reson.* **2001**, *153*, 48–55.

[22] The X-ray volume ($V_{X\text{-}ray}$) was calculated by dividing the crystallographic unit-cell volume by the number of molecular entities (assumed to have a spherical shape) contained in the unit cell and subtracting the van der Waals volumes of the counterions: Y. H. Zhao, M. H. Abraham, A. M. Zissimos, *J. Org. Chem.* **2003**, *68*, 7368–7373.

[23] E. J. Cabrita, S. Berger, *Magn. Reson. Chem.* **2002**, *40*, S122–S127.

[24] a) A. M. Aguiar, J. Beislar, *J. Org. Chem.* **1964**, *29*, 1660–1662; b) R. P. K. Babu, S. S. Krishnamurthy, M. Nethaji, *Tetrahedron: Asymmetry* **1995**, *6*, 427–438; c) J. J. Bishop, A. Davidson, M. L. Katcher, D. W. Lichtenberg, R. E. Merrill, J. C. Smart, *J. Organomet. Chem.* **1971**, *27*, 241–249.

[25] *Collect* data collection software, Bruker AXS, Delft, The Netherlands. **2004**.

[26] Z. Otwinowski, W. Minor, *Methods Enzymol.* **1997**, *276*, 307–326.

[27] R. H. Blessing, *Acta Crystallogr., Sect. A* **1995**, *51*, 33–38.

[28] *CrysAlis^{Pro} CCD*, *CrysAlis^{Pro} RED*, Oxford Diffraction Ltd., Abingdon, Oxfordshire, UK, **2008**.

[29] L. J. Farrugia, *J. Appl. Crystallogr.* **1999**, *32*, 837–838.

[30] P. T. Beurskens, G. Admiraal, G. Beurskens, W. P. Bosman, S. García-Granda, R. O. Gould, J. M. M. Smits, C. Smykalla, *The DIRDIF Program System*, Technical Report of the Crystallographic Laboratory, University of Nijmegen, The Netherlands, **1999**.

[31] G. M. Sheldrick, *SHELXL97: Program for the Refinement of Crystal Structures*, University of Göttingen, Germany, **1997**.

[32] *International Tables for X-ray Crystallography*, Kynoch Press, Birmingham, U. K., **1974**, vol. IV (present publisher: Kluwer Academic Publishers, Dordrecht, The Netherlands).
[33] M. Nardelli, *Comput. Chem.* **1983**, *7*, 95–98.
[34] A. L. Spek, *PLATON: A Multipurpose Crystallographic Tool*, University of Utrecht, The Netherlands, **2007**.
Received: September 13, 2010
Published Online: December 9, 2010

